Effects of organic polymer addition in magnetite synthesis on its crystalline structure

doi: https://doi.org/10.1039/C4RA02073A

Effects of organic polymer addition in magnetite synthesis on its crystalline structure

Yoshimitsu Kuwahara[1], Toshiki Miyazaki[1], Yuki Shirosaki[2] and Masakazu Kawashita[3]

[1]Graduate School of Life Science and System Engineering, Kyushu Institute of Technology, Kitakyushu, Japan

[2]Frontier Research Academy for Young Researchers, Kyushu Institute of Technology, Kitakyushu, Japan

[3]Graduate School of Biomedical Engineering, Tohoku University, Sendai, Japan

*Corresponding author: Associate Professor Toshiki Miyazaki

2-4, Hibikino, Wakamatsu-ku, Kitakyushu 808-0196, Japan

Tel.: +81-93-695-6025

Fax: +81-93-695-6025

E-mail: tmiya@life.kyutech.ac.jp

Summary

Magnetite (Fe_3O_4) nanoparticles and magnetite-based inorganic-organic hybrids are attracting attention in biomedical fields as thermoseeds for hyperthermia and contrast medium in magnetic resonance imaging. Size control of Fe_3O_4 thermoseeds is important as the particle size affects the heat generation properties. Fe_3O_4 can be easily synthesized via aqueous processes and the presence of organic substances during synthesis can affect the size and crystalline phase of the Fe_3O_4 formed. In this study, various polymers with different functional groups and surface charges were added to the precursor solution of Fe_3O_4 to clarify the relationship between the chemical structure of the organic substances and the crystal structure of Fe_3O_4. At first, coexistence effects of the organic substances in the solutions were clarified. As a result, crystalline Fe_3O_4 was precipitated even after addition of neutral polyethylene glycol and cationic poly(diallyldimethylammonium chloride). The poly(sodium-4-styrene sulfonate) addition significantly decreased the particle size, while polyacrylic acid addition inhibited Fe_3O_4 nucleation to afford amorphous phase. These differences were related to the ease of complex formation from iron ions and coexisting organic polymers. In order to clarify this assumption, modified experimental procedure was applied for the polyacrylic acid. Namely, the iron oxide precipitation by NaOH solution was followed by the polyacrylic acid addition. Notably, Fe_3O_4 nucleation was not inhibited. Hence, the size and crystalline phase of the iron oxide prepared by the aqueous process were drastically affected by organic polymers.

Keywords: Magnetite, Organic polymer, Crystalline phase, Complex formation

Introduction

Magnetite (Fe_3O_4) is an industrially important ceramic for magnetic applications, electric applications and in biomedical fields (e.g. as thermoseeds for hyperthermia treatments). Hyperthermia is a cancer treatment with low invasion, based on the cancer cells having lower heat resistivity than normal cells [1]. The tumour is heated by techniques, such as infrared radiation, radiofrequency ablation and hot water treatment. However, the tumours located deep inside the body cannot be effectively treated, because the tumour is heated from outside the body in these techniques. Hence, novel cancer treatments using ferromagnetic ceramic particles such as Fe_3O_4 and γ-hematite (γ-Fe_2O_3) are attracting much attention. The deep-seated tumours can be heated effectively and killed if ferromagnetic ceramic particles are implanted around the tumours and an alternating magnetic field is applied. Various magnetic nanoparticles have been investigated as thermoseeds for this process [2,3]. Moreover, implantation of ferromagnetic microspheres with 20–30 μm size in blood vessels around the tumours can exhibit the hyperthermia and embolization effect to cut off the nutrition supply to the tumours [4–6].

Inorganic-organic hybrids comprising Fe_3O_4 and anionic carboxymethyl dextran (CM-dextran) have been used clinically as contrast media for magnetic resonance imaging (MRI) [7,8] and thermoseeds for hyperthermia [9,10]. CM-dextran is known to be biologically compatible [11], and iron ions have low cell toxicity compared to other the metal ions [12]. In the preparation of inorganic-organic hybrids, the chemical structure or molecular weight of the added polymer affects the ionic interaction between polymer and iron salts as well as the grain size and morphology of the prepared Fe_3O_4 core [13,14]. The heat generation properties are drastically dependent on the particle size

of the Fe_3O_4 nanoparticles, because Fe_3O_4 converts from ferromagnetic into superparamagnetic with a decrease in particle size [15,16]. The *in situ* precipitation of Fe_3O_4 with 13 μm average diameter particles in cationic chitosan hydrogels [17] and the crystal phase control of the iron oxide were attempted in an aqueous solution with ethylenediaminetetraacetic acid [18]. Also, preparation of Fe_3O_4 nanoparticles modified with poly(diallyldimethylammonium chloride) (PDDAC) has been also reported [19]. These studies suggest that organic-inorganic interaction affects the nanostructure and properties of Fe_3O_4-polymer hybrids. However, the effects of coexistence of different functional groups in the added organic substances on the crystalline structure and particle size of the iron oxide have not been investigated in detail. Hence, the fundamental knowledge beneficial for the design of Fe_3O_4-based hybrids with various magnetic properties could be gained with further investigations. Clarification of this point is important in order to facilitate simple one-pot synthesis of the hybrids.

In the present study, Fe_3O_4 nanoparticles were synthesized using an aqueous process with the addition of various organic polymers with different functional groups and surface charges, such as polyacrylic acid (PAA), poly(sodium-4-styrene sulfonate) (PSS), polyethylene glycol (PEG) and PDDAC. This study was performed to clarify the relationship between the chemical structure of the added polymer and the resulting crystalline structure of the iron oxide nanoparticles. Effects of sequence of the polymer addition on crystalline structure of the resultant nanoparticles were also investigated.

Materials and Methods

Iron (II) chloride tetrahydrate, iron (III) chloride hexahydrate, PAA (Mw = 25,000) and PEG (Mw = 20,000) were purchased from Wako Pure Chemical Industries,

Japan. NaOH was supplied by Nacalai Tesque, Japan and PSS (Mw = 1,000,000) and PDDAC (Mw = 100,000–200,000) were purchased from Sigma Aldrich, USA. In this study, two types of aqueous preparation processes were undertaken. For Method 1, the procedure is as follows: 1) 25 mL of 50 mM iron (II) chloride and 98 mM iron (III) aqueous solution was prepared. 2) PAA, PSS, PEG and PDDAC were then dissolved in the solution at 4 mass%. 3) 1 M NaOH aqueous solution was added dropwise to the solution up to pH 7. NaOH solution about 12 to 25 mL was used for the neutralization for each specimen. 4) The solution was stirred at 75°C for 1 h to precipitate the solid particles. 5) To remove excessive water soluble by-products the solution was dialyzed using a cellulose tube for 24 h and the precipitates formed were filtered. The obtained powder was finally dried at 60°C for 24 h.

In Method 2, the sequence of the polymer addition was different from that in Method 1. Namely, the iron chloride solution was added with 1 M NaOH solution, stirred at 75°C for 1 h, and subsequently added to the polymer. The removal procedure for the by-products obtained was same as Method 1.

The analysis of the crystal structure of the obtained product was performed using powder X-ray diffraction (XRD, MXP3V, Mac Science Ltd., Japan). The morphology of the products was observed using a transmission electron microscope (TEM, H-9000NAR, Hitachi Co., Japan) and the particle size distribution was measured from the TEM photographs. For TEM observation, the samples were dispersed in ultrapure water, put on carbon support films (ELS-C10, Okenshoji Co., Ltd., Japan) and then dried at room temperature for 24 h. Thermal properties of the obtained specimens were analysed by thermogravimetry / differential thermal analyzer (TG-DTA, Model 2000S, Mac Science Ltd., Japan). The samples were heated at 800°C in a Pt sample pan at rate of 5°C/min. The

crystalline size of the obtained particles (D) was also calculated by using Scherrer's equation [20]:

$$D = \frac{0.9\lambda}{B\cos\theta_B} \qquad (1)$$

where λ, B, θ_B correspond to the wavelength (0.154 nm), half width of (311) diffraction of the magnetite, and the (311) diffraction angle, respectively, of the X-ray.

Results and Discussion

It was confirmed by TG-DTA that the samples obtained by Method 1 showed mass reduction by 30 - 90 % due to thermal decomposition of the polymers (data not shown), meaning that they take a form of organic-inorganic hybrid. Figure 1 shows XRD patterns of the samples prepared by Method 1. Peaks assigned to crystalline Fe_3O_4 (JCPDS#19-0629) were detected for the samples with PEG, PDDAC and PSS as well as for samples without a polymer. In the case of PSS, the peaks detected were much broader than the other samples. Broad halo pattern assigned to amorphous phase was only observed for the sample with PAA. Peaks assigned to PEG (JCPDS#49-2109) were observed for the sample with PEG. In addition, small peaks assigned to NaCl formed by reaction of iron chloride and NaOH were observed for some specimens. However adverse effects for the body might be small in medical application, because NaCl is highly abundant in body fluid.

Figure 2 shows TEM photographs and the size distributions of the samples prepared by Method 1. All samples have a dispersion of size between 5 and 30 nm. The average particle size of the samples with PEG and PDDAC was almost similar to that

without a polymer. On the contrary, the particle size distribution of the sample with PSS shifted to much smaller values and the average particle size significantly decreased.

The above results suggest that coexistence of PAA in iron ion solution significantly inhibit Fe_3O_4 formation. In order to clarify this assumption, Method 2 was applied for PAA. Figure 3 shows XRD patterns of the sample with PAA prepared by Method 2. Unlike Method 1, peaks assigned to Fe_3O_4 were detected even after PAA addition.

Figure 4 shows TEM photographs and size distributions of the sample with PAA prepared by Method 2. The average particle size was much smaller than the sample without a polymer as shown in figure 2.

Table 1 shows crystalline size of the specimens calculated by Scherrer's equation. The crystalline size showed tendency to decrease by the polymer addition. This coincided with the results of TEM observation in figure 4.

The present results indicate that Fe_3O_4 nanoparticles modified with organic polymers were obtained even at neutral conditions. From the aqueous synthesis by Method 1, it was determined that crystalline phase and particle size of the iron oxide were significantly affected by the type of organic polymer added. It is known that the Fe_3O_4 formation progresses through the following reactions with Fe^{2+} and Fe^{3+} as precursors [21,22]:

$$Fe^{2+} + 2OH^- \rightarrow Fe(OH)_2 \quad (2)$$

$$Fe^{3+} + 3OH^- \rightarrow Fe(OH)_3 \quad (3)$$

$$Fe(OH)_3 \rightarrow FeOOH + H_2O \quad (4)$$

$$Fe(OH)_2 + 2FeOOH \rightarrow Fe_3O_4 + 2H_2O \quad (5)$$

In the case of PAA-added specimen, most of the added NaOH would be consumed for neutralization of PAA. This is supported by the fact that larger amount of NaOH solution was needed for completion of the reaction. The ionic activity of the iron ions may have decreased considering the strong ionic interaction that occurs between the iron ions and the negatively-charged carboxyl group in polyacrylate ions to form a complex. Formation of the iron polyacrylate by reaction between the polyacrylate ions and iron ions was previously confirmed by a peak shift of the asymmetric stretching of the carboxylate ion (COO^-) in FT-IR spectra [23,24]. It is considered that Fe^{2+} in the complex is oxidized by the dissolved O_2 before reaction with OH^- and that $Fe(OH)_2$ as an essential intermediate of Fe_3O_4 was not sufficiently generated. Despite PSS also being negatively charged, it did not inhibit the Fe_3O_4 nucleation (figure 1). It has been reported that the stability constants of the complex of $Fe(CH_3COO)^{2+}$ and $FeSO_4^+$ are $10^{3.38}$ and $10^{2.56}$, respectively [25,26]. This means that $FeSO_4^+$ is less stable than $Fe(CH_3COO)^{2+}$. Therefore, it is assumed that subsequent iron hydroxide formation afforded Fe_3O_4 as a final product.

However, the PSS addition afforded much smaller Fe_3O_4 particles in comparison with other polymers (figure 3). It is assumed that negatively-charged PSS adsorbs on the positively-charged magnetite nuclei via ionic interaction and inhibits its crystal growth. A similar interaction is also observed on Fe_3O_4 nanoparticles modified with CM-dextran, poly(ethylene imine) and chitosan [9,27].

In contrast, for neutral PEG and cationic PDDAC, inhibition of Fe_3O_4 nucleation and Fe_3O_4 growth was hardly observed (figures 1 and 2). An electric repulsion between the iron ions and the polymer could contribute to the vigorous Fe_3O_4 formation.

In Method 2, Fe_3O_4 was formed even by PAA addition (figure 3). Hence, Fe_3O_4 nucleation was almost complete when the polymers were added to the solution. However, the particle size was much smaller than that without polymer addition (figure 4). Hence, crystal growth was inhibited by the subsequent polymer addition. Adsorption of the added PAA onto the magnetite nuclei by ionic interaction would inhibit the crystal growth similar to PSS addition by Method 1. Molecular weight of PSS was much higher than other polymer additives used in this study. The additives with high molecular weight may increase viscosity of the solution and hence significantly retard the Fe_3O_4 growth. Effect of the molecular weight should be further examined in future study.

Conclusions

Iron oxide nanoparticles were synthesized in the presence of various polymers in an aqueous process. The crystalline phase and size of the nanoparticles were affected by the type of polymer added and also the sequence of the polymer addition. Hence, the interaction between the precursor iron ions and the functional groups in the polymers affect the crystalline structure of the resulting particles. In the present study, the results obtained provide fundamental knowledge on magnetite particles modified with organic substances with different crystalline structures. Magnetic properties of the obtained particles should be evaluated in the next step.

Acknowledgments

This work was supported by a Grant-in-Aid for Scientific Research on Innovative Areas, ‘Fusion Materials: Creative Development of Materials and Exploration of Their Function

through Molecular Control' (No. 2206) from the Ministry of Education, Culture, Sports, Science and Technology, Japan (MEXT).

References

[1] Conway, J. & Anderson, A. P. 1986 Electromagnetic techniques in hyperthermia. *Clin*. *Phys*. *Physiol*. *Meas*. **7**, 287-318 (DOI:10.1088/0143-0815/7/4/001).

[2] Jeyadevan, B. 2010 Present status and prospects of magnetite nanoparticles-based hyperthermia. *J. Ceram. Soc. Jpn.* **118**, 391-401 (DOI: 10.2109/jcersj2.118.391).

[3] Kobayashi, T. 2011 Cancer hyperthermia using magnetic nanoparticles. *Biotechnol. J.* **6**, 1342-1347 (DOI: 10.1002/biot.201100045).

[4] Day, E. 1993 Radiotherapy glasses. In: *An Introduction to Bioceramics* (ed. L. L. Hench & J. Wilson), pp. 305-317. Singapore: World Scientific.

[5] Kawashita, M. 2005 Ceramic microspheres for biomedical applications. *Int. J. Appl. Ceram*. *Technol.* **2**, 173-183 (DOI: 10.1111/j.1744-7402.2005.02023.x).

[6] Miyazaki, T., Miyaoka, A., Ishida, E., Li, Z., Kawashita, M. & Hiraoka, M. 2012 Preparation of ferromagnetic microcapsules for hyperthermia using water/oil emulsion as a reaction field. *Mater. Sci. Eng., C* **32**, 692-696 (DOI: 10.1016/j.msec.2012.01.010).

[7] Josephson, L. 2006 Magnetic nanoparticles for MR imaging. In: *BioMEMS and Biomedical Nanotechnology: Volume I: Biological and Biomedical Nanotechnology* (ed. M. Ferrari, A. P. Lee & L. J. Lee), pp. 227-237. Berlin: Springer.

[8] Hong, R.Y., Feng, B., Chen, L. L., Liu, G. H., Li, H. Z., Zheng, Y. & Wei, D. G. 2008 Synthesis, characterization and MRI application of dextran-coated Fe_3O_4 magnetic nanoparticles. *Biochem. Eng. J.* **42**, 290-300 (DOI: 10.1016/j.bej.2008.07.009).

[9] Mitsumori, M., Hiraoka, M., Shibata, T., Okuno, Y., Masunaga, S., Koishi, M., Okajima, K., Nagata, Y., Nishimura, Y., Abe, M. et al. 1994 Development of intra-arterial hyperthermia using a dextran-magnetite complex. *Int. J. Hyperthermia* **10**, 785-793 (DOI:10.3109/02656739409012371).

[10] Mitsumori, M., Hiraoka, M., Shibata, T., Okuno, Y., Nagata, Y., Nishimura, Y., Abe, M., Hasegawa, M., Nagae, H. & Ebisawa Y. 1996 Targeted hyperthermia using dextranmagnetite complex: a new treatment modality for liver tumors. *Hepato–Gastroenterology* **43**, 1431-1437.

[11] Shahnaz, G., Perera, G., Sakloetsakun, D., Rahmat, D. & Bernkop-Schnürch, A. 2010 Synthesis, characterization, mucoadhesion and biocompatibility of thiolated carboxymethyl dextran–cysteine conjugate. *J. Controlled Release* **144**, 32-38 (DOI: 10.1016/j.jconrel.2010.01.033).

[12] Yamamoto, A., Honma, R. & Sumita, M. 1998 Cytotoxicity evaluation of 43 metal salts using murine fibroblasts and osteoblastic cells. *J. Biomed. Mater. Res*. **39**, 331-340 (DOI: 10.1002/(SICI)1097-4636(199802)39:2<331::AID-JBM22>3.0.CO;2-E).

[13] Kawaguchi, T., Hanaichi, T., Hasegawa, M. & Maruno S. 2001 Dextran-magnetite complex: conformation of dextran chains and stability of solution. *J. Mater. Sci.: Mater. Med*. **12**, 121-127 (DOI: 10.1023/A:1008961709559).

[14] Kawaguchi, T. & Hasegawa, M. 2000 Structure of dextran–magnetite complex: relation between conformation of dextran chains covering core and its molecular weight. *J. Mater. Sci.: Mater. Med*. **11**, 31-35 (DOI: 10.1023/A:1008933601813).
[15] Li, Z., Kawashita, M., Araki, N., Mitsumori, M. & Hiraoka M. 2009 Preparation of size-controlled magnetite nanoparticles for hyperthermia of cancer. *Trans. Mater. Res. Soc. Jpn.* **34**, 77-80.
[16] Li, Z., Kawashita, M., Araki, N., Mitsumori, M., Hiraoka, M. & Doi, M. 2010 Magnetite nanoparticles with high heating efficiency for application in hyperthermia of cancer. *Mater. Sci. Eng., C* **30**, 990-996 (DOI: 10.1016/j.msec.2010.04.016).
[17] Wang, Y., Li, B., Zhou, Y. & Jia, D. 2009 In situ mineralization of magnetite nanoparticles in chitosan hydrogel. *Nanoscale. Res. Lett*. **4**, 1041-1046 (DOI: 10.1007/s11671-009-9355-1).
[18] Oaki, Y., Yagita, N. & Imai, H. 2012 One-Pot aqueous solution syntheses of Iron Oxide nanostructures with controlled crystal phases through a microbial-mineralization-inspired approach. *Chem*. *Eur*. *J.* **18**, 110-116 (DOI: 10.1002/chem.201102663).
[19] Yu CJ, Lin CY, Liu CH, Cheng TL & Tseng WL. 2010 Synthesis of poly(diallyldimethylammonium chloride)-coated Fe_3O_4 nanoparticles for colorimetric sensing of glucose and selective extraction of thiol. *Biosens. Bioelectron*., **26**, 913-917 (DOI: 10.1016/j.bios.2010.06.069).
[20] Stock S. R., 2001 *Elements of X-ray diffraction, 3rd ed*., New Jersey: Prentice Hall.
[21] Lian, S., Wang, E., Kang, Z., Bai, Y., Gao, L., Jiang, M., Hu, C. & Xu, L. 2004 Synthesis of magnetite nanorods and porous hematite nanorods. *Solid State Commun*. **129**, 485-490 (DOI: 10.1016/j.ssc.2003.11.043).
[22] Mahmoudi, M., Simchi, A., Imani, M., Milani, A. S. & Stroeve, P. 2008 Optimal design and characterization of superparamagnetic Iron Oxide nanoparticles coated with polyvinyl alcohol for targeted delivery and imaging. *J. Phys. Chem. B* **112**, 14470-14481 (DOI: 10.1021/jp803016n).
[23] Kamitakahara, M., Kim, H.-M., Miyaji, F., Kokubo, T. & Nakamura, T. 2000 Preparation of Al-free glass-ionomer cement. *J. Ceram. Soc. Jpn.* **108**, 1117-1118 (DOI: 10.2109/jcersj.108.1264_1117).
[24] Kirwan, L. J., Fawell, P. D. & van Bronswijk, W. 2003 In situ FTIR-ATR examination of poly(acrylic acid) adsorbed onto hematite at low pH. *Langmuir* **19**, 5802-5807 (DOI: 10.1021/la027012d).
[25] Martell, A. E. & Smith, R. M. 1975 *Critical Stability Constants*. New York: Plenum Press.
[26] Kanroji, Y. 1963 Studies on the complex ions in mineral springs. II. Stability constants of Iron (III) Sulfate and Chloride complexes. *Yakugaku Zasshi* **83**, 424-427 (in Japanese).
[27] Veiseh, O., Gunn, J. W. & Zhang, M., 2010 Design and fabrication of magnetic nanoparticles for targeted drug delivery and imaging, *Adv*. *Drug Deliv. Rev*., **62**, 284-304 (DOI: 10.1016/j.addr.2009.11.002).

Figure captions

Figure 1. XRD patterns of the samples prepared by Method 1.

Figure 2. TEM micrographs and particle size distribution of the samples prepared by Method 1.

Figure 3. XRD pattern of the sample with added PAA prepared by Method 2.

Figure 4. TEM micrographs and particle size distribution of the sample with added PAA prepared by Method 2.

Table 1 Crystalline size of the specimens calculated by Scherrer's equation

Polymer additive	*D* / nm
None	11.6
PSS (Method 1)	7.3
PEG (Method 1)	14.4
PDDAC (Method 1)	10.2
PAA (Method 2)	8.0

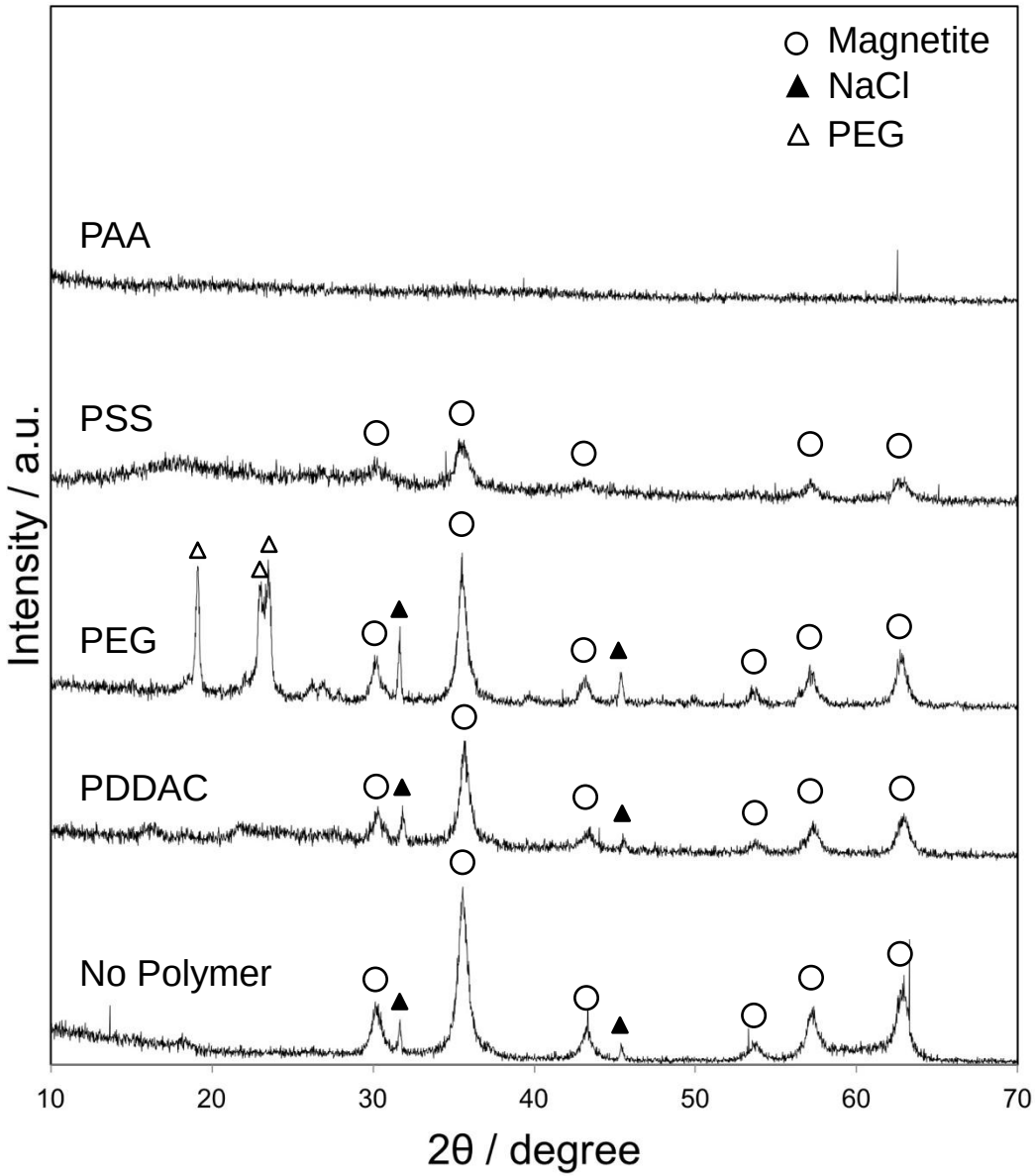

Kuwahara et al.
Fig. 1

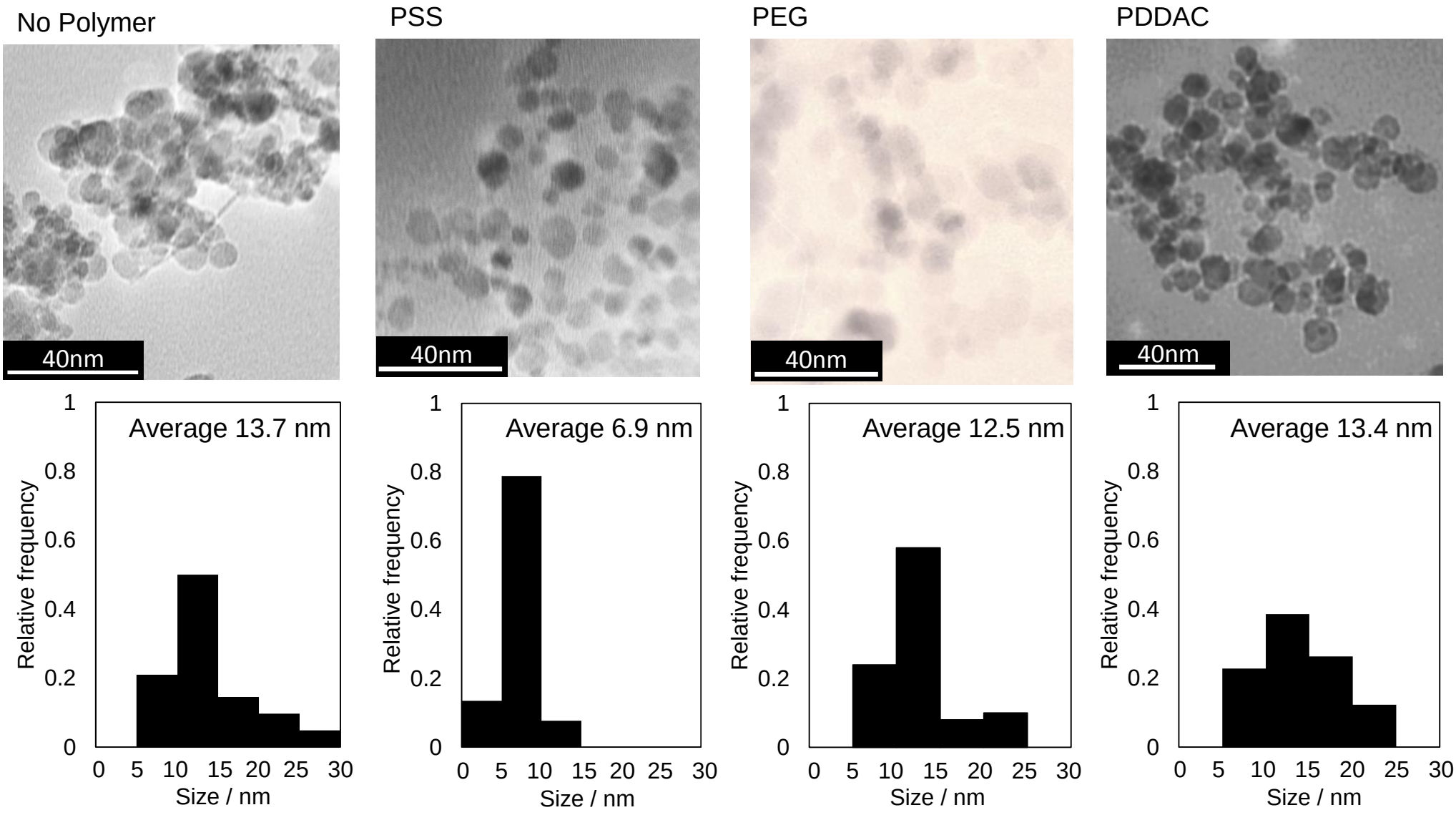

Kuwahara et al.
Fig. 2

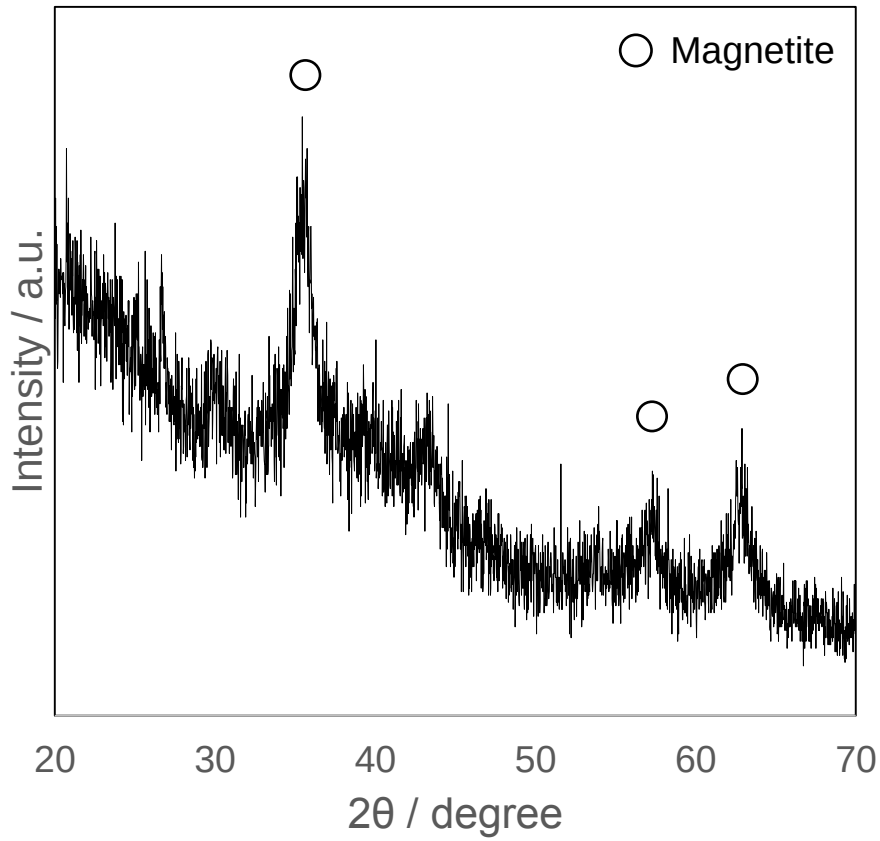

Kuwahara et al.
Fig. 3

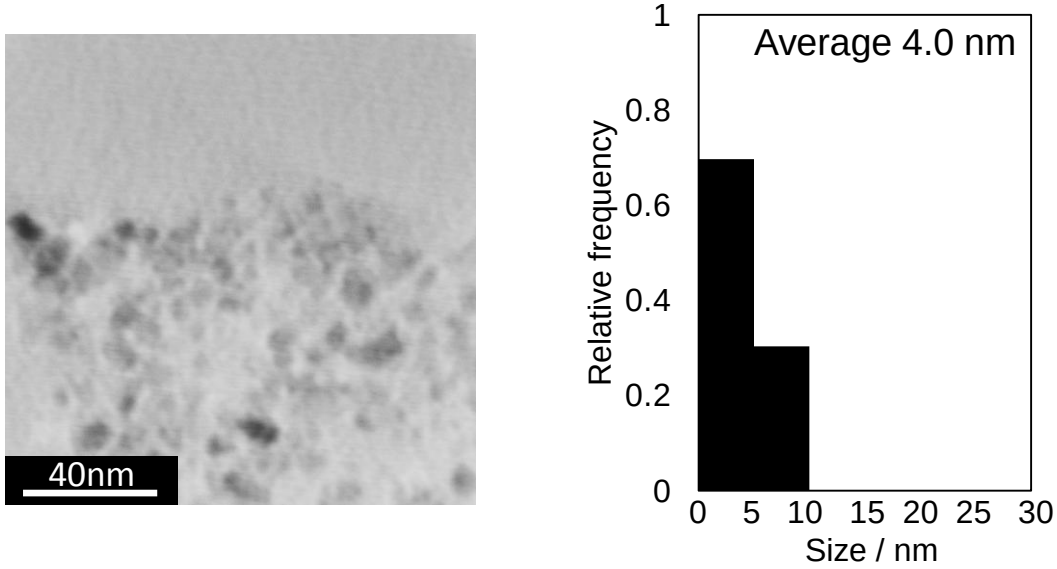

Kuwahara et al.
Fig. 4